In vivo antitumor activity of NVP-AEW541—A novel, potent, and selective inhibitor of the IGF-IR kinase

Carlos García-Echeverría,[1] Mark A. Pearson,[1] Andreas Marti,[1] Thomas Meyer,[1] Juergen Mestan,[1] Johann Zimmermann,[1] Jiaping Gao,[2] Josef Brueggen,[1] Hans-Georg Capraro,[1] Robert Cozens,[1] Dean B. Evans,[1] Doriano Fabbro,[1] Pascal Furet,[1] Diana Graus Porta,[1] Janis Liebetanz,[1] Georg Martiny-Baron,[1] Stephan Ruetz,[1] and Francesco Hofmann[1,*]

[1]Novartis Institutes for BioMedical Research, Novartis Pharma AG, CH-4002 Basel, Switzerland
[2]Novartis Institutes for BioMedical Research, Inc., Cambridge, Massachusetts 02138
*Correspondence: francesco.hofmann@pharma.novartis.com

Summary

IGF-IR-mediated signaling promotes survival, anchorage-independent growth, and oncogenic transformation, as well as tumor growth and metastasis formation in vivo. NVP-AEW541 is a pyrrolo[2,3-*d*]pyrimidine derivative small molecular weight kinase inhibitor of the IGF-IR, capable of distinguishing between the IGF-IR (IC_{50} = 0.086 μM) and the closely related InsR (IC_{50} = 2.3 μM) in cells. As expected for a specific IGF-IR kinase inhibitor, NVP-AEW541 abrogates IGF-I-mediated survival and colony formation in soft agar at concentrations that are consistent with inhibition of IGF-IR autophosphorylation. In vivo, this orally bioavailable compound inhibits IGF-IR signaling in tumor xenografts and significantly reduces the growth of IGF-IR-driven fibrosarcomas. Thus, NVP-AEW541 represents a class of selective, small molecule IGF-IR kinase inhibitors with proven in vivo antitumor activity and potential therapeutic application.

Introduction

The insulin-like growth factor I receptor (IGF-IR) is a tetrameric transmembrane receptor tyrosine kinase composed of two α and two β subunits linked by disulfide bonds. The extracellular α subunit is responsible for ligand binding, whereas the β subunit consists of a transmembrane domain and a cytoplasmic tyrosine kinase domain (for review, see Ullrich and Schlessiger, 1990; Van der Geer et al., 1994). The receptor is primarily activated by its cognate ligands, insulin-like growth factor I (IGF-I) and II (IGF-II; 2- to 15-fold lower affinity), and, albeit at a much lower affinity (500- to 1000-fold less), by insulin. Ligand binding activates the intrinsic tyrosine kinase activity, resulting in trans-β subunit autophosphorylation and stimulation of signaling cascades that include the IRS-1/PI-3K/PKB/S6K and Grb2/Sos/Ras/MAPK pathways. Activation of the IGF-IR has been reported to result in proliferation, survival, transformation, metastasis, and angiogenesis (for review, see Baserga, 2000; Wang and Sun, 2002).

Extensive studies have demonstrated that IGF-I acts as a mitogen both in vitro and in vivo. In fact, IGF-I, together with PDGF, was originally shown to be essential for the proliferation of fibroblasts in vitro (Stiles et al., 1979). Downregulation of IGF-IR function, by either gene disruption (Sell et al., 1994), antisense oligonucleotides (White et al., 2000), neutralizing antibodies (Artega and Osborne, 1989; De Leon et al., 1992), or dominant negative mutants (Prager et al., 1994; D'Ambrosio et al., 1996; Reiss et al., 1998), was found to interfere with cell growth and proliferation. In particular, IGF-I signaling was demonstrated to play a vital role in cellular transformation. Overexpression of the IGF-IR is sufficient to transform immortalized mouse fibroblasts, as assayed by survival and growth in soft agar and the formation of tumors in nude mice (Kaleko et al., 1990), whereas fibroblasts genetically deficient for the IGF-IR gene are resistant to transformation by SV40 T antigen, c-Src, Ras, PDGFR, or EGFR (Sell et al., 1993, 1994; Coppola et al., 1994; De Angelis et al., 1995; Valentinis et al., 1997).

Several experimental approaches have demonstrated the therapeutic potential of interfering with IGF-IR-mediated signaling in vivo. Inhibition of primary tumor growth was achieved with IGF-IR blocking antibodies (Scotlandi et al., 1998), upon overexpression of a dominant negative mutant (Reiss et al., 1998; Prager et al., 1994; D'Ambrosio et al., 1996; Kalebic et al., 1998; Li et al., 2000; Scotlandi et al., 2002a), as well as by means of antisense cDNA or oligonucleotides to downregulate IGF-IR expression (Resnicoff et al., 1994, 1995; Shapiro et al., 1994; Nakamura et al., 2000). Additional antisense studies suggested an important role for IGF-IR in invasion and metastasis formation (Long et al., 1995; Burfeind et al., 1996; Dunn et al., 1998; Chernicky et al., 2000; Samani et al., 2001; Scotlandi

SIGNIFICANCE

Insulin-like growth factors and their receptor tyrosine kinase, IGF-IR, have been implicated in the development and progression of cancer, by contributing proliferative, antiapoptotic, transforming, and proangiogenic signaling. The clinical development of the orally bioavailable, selective, small molecule kinase inhibitor of the IGF-IR, NVP-AEW541, will provide the unique opportunity to perform clinical proof-of-concept studies to test this novel therapeutic strategy in oncology.

et al., 2002b). This hypothesis was further reinforced by the enhanced transition to invasive carcinoma and formation of metastases observed upon targeted overexpression of the IGF-IR in the RipTag model of pancreatic carcinogenesis (Lopez and Hanahan, 2002).

Epidemiological evidence for a role of IGF-IR signaling in cancer has emerged from various studies demonstrating increased expression levels of multiple components of the IGF signaling system in diverse tumor types (for review, see Yu and Rohan, 2000; Khandwala et al., 2000; Grimberg and Cohen, 2000; Fürstenberger and Senn, 2002).

Based on the evidence described above, a drug discovery program to identify and develop a potent and selective small molecular mass inhibitor of the IGF-IR signaling pathway as an anticancer agent was initiated. A major hurdle to this approach is the close homology of the IGF-IR and the InsR kinase domains. The ATP binding site of these two receptors displays 100% sequence identity, whereas the entire kinase domains share 84% sequence identity, both with each other and across species.

Hereafter, we describe the in vitro and in vivo characterization of a potent IGF-IR kinase inhibitor capable of selectively inhibiting IGF-IR kinase activity, as opposed to InsR kinase activity, at the cellular level, and significantly reducing the growth of IGF-IR-driven fibrosarcomas.

Table 1. In vitro inhibitory activity and selectivity of NVP-AEW541

Enzyme	IC_{50} [μM] ± SEM	n	Kinase type
IGF-IR	0.15 ± 0.036	6	Tyr
Ins-R	0.14 ± 0.039	5	Tyr
HER-1	5.8 ± 1.4	4	Tyr
HER-2	4.1 ± 1.4	5	Tyr
HER-4	1.4 ± 0.41	2	Tyr
KDR	2.3 ± 0.24	5	Tyr
Tek	0.53 ± 0.22	3	Tyr
PDGFR	2.0 ± 0.61	3	Tyr
c-Met	3.8 ± 1.0	4	Tyr
c-Abl	>10	5	Tyr
c-Src	2.4 ± 0.38	3	Tyr
c-Kit	3.3 ± 1.4	3	Tyr
Flt-4	2.4 ± 0.46	3	Tyr
Flt-1	0.60 ± 0.13	3	Tyr
Flt-3	0.42 ± 0.11	6	Tyr
FGFR-1	4.1 ± 1.1	4	Tyr
PKB	>10	4	Ser/Thr
Cdk1/Cyc.B	>10	3	Ser/Thr
PDK1	4.8 ± 2.1	4	Ser/Thr
c-Raf-1	>10	3	Ser/Thr
PKA	>10	3	Ser/Thr

In vitro kinase assays were performed with the indicated purified kinases/recombinant kinase domains in the absence or presence of increasing concentrations of NVP-AEW541, as described in the Experimental Procedures. IC_{50}s are expressed as means ± SEM. The number of independent IC_{50} determinations is indicated with n. Tyr: tyrosine-specific protein kinase. Ser/Thr: serine/threonine-specific protein kinase.

Results

Small molecules belonging to the pyrrolo[2,3-*d*]pyrimidine class were identified in a high-throughput screening of our in-house compound archive as inhibitors of the IGF-IR in vitro kinase activity. This compound class was subjected to a medicinal chemistry program aimed at optimizing the potency and selectivity toward the IGF-IR kinase, as well as their drug-like properties. NVP-AEW541 is a representative example of such an optimization process, whose potency and selectivity was first assessed in a series of in vitro kinase assays using different recombinant kinase domains or purified kinases and synthetic peptide substrates (Table 1). The compound was found to inhibit the in vitro kinase activity of the recombinant IGF-IR kinase domain with an IC_{50} value of 0.15 μM and to be equipotent against the recombinant InsR kinase domain. NVP-AEW541 displayed at least 10-fold selectivity toward the IGF-IR, as compared to most of the other kinases tested. The only exceptions were represented by the Flt-1, Flt-3, and Tek kinases, where the compound inhibited the respective recombinant kinase domains with IC_{50} values 3- to 4-fold higher than those measured for the IGF-IR.

In order to assess the ability of NVP-AEW541 to inhibit its target in cells, and to test the selectivity of the compound against a panel of native tyrosine kinases (IGF-IR, InsR, HER-1, PDGFR, c-Kit, Bcr-Abl), their autophosphorylation was measured in the presence or absence of the compound (Table 2). NVP-AEW541 was confirmed active toward the IGF-IR kinase (IC_{50} = 0.086 μM) and shown to be selective at the cellular level. Indeed, NVP-AEW541 was found to be 27-fold more potent toward the native IGF-IR, as compared to the structurally related native InsR. The selectivity observed at the cellular level indicates that, despite the 84% identity of the IGF-IR and InsR kinase domains, there are conformational differences between the native forms of these receptor tyrosine kinases that are not recapitulated by the recombinant kinase domains used in the in vitro kinase assay. Thus, at the cellular level, NVP-AEW541 is highly selective against the IGF-IR, as compared to both the InsR and other tyrosine kinases.

Given the survival function that has been ascribed to IGF-IR-mediated signaling and the requirement of IGF-IR mediated signaling for cellular transformation, the ability of the compound to inhibit IGF-I-mediated survival of MCF-7 cells in the absence of serum and to prevent their ability to grow in an anchorage-independent manner was analyzed. NVP-AEW541 was shown to inhibit IGF-I-mediated survival of MCF-7 cells (Table 3), as well as their ability to grow in soft agar (Table 3), at concentrations consistent with its capacity to inhibit receptor autophosphorylation (data not shown).

As an effective therapeutic agent, NVP-AEW541 must also be able to inhibit IGF-I-stimulated signaling (Figure 1) and proliferation in the presence of serum (Table 3). The cell line selected for these tests, NWT-21, is a NIH3T3 derivative that stably ex-

Table 2. Cellular inhibitory activity and selectivity of NVP-AEW541

Enzyme	IC_{50} (μM) ± SEM	n
IGF-IR	0.086 ± 0.028	5
InsR	2.3 ± 0.163	2
HER1	>10	1
PDGFR	>10	1
c-Kit	>5	2
Bcr-Abl p210	>10	1

The autophosphorylation of the indicated kinases was determined at the cellular level in the absence or presence of increasing concentrations of NVP-AEW541. IC_{50}s are expressed as means ± SEM and the number of independent determinations is indicated with n.

Table 3. Inhibition of IGF-I-mediated survival, anchorage-independent growth, and cellular proliferation by NVP-AEW541

Assay	Cell line	IC_{50} (μM) ± SEM	n
IGF-I-mediated survival	MCF-7	0.162 ± 0.016	8
Soft agar	MCF-7	0.105 ± 0.018	2
Proliferation	NWT-21	1.64 ± 0.67	6

The ability of NVP-AEW541 to inhibit IGF-I-mediated survival was assessed in MCF-7 cells in the absence of serum. Inhibition of anchorage-independent growth by NVP-AEW541 was assessed in a soft agar assay using MCF-7 cells. The proliferative capacity of NWT-21 cells (NIH3T3 stably expressing the human IGF-IR) growing in serum-containing media was determined in the absence and presence of increasing concentrations of the compound. The IC_{50} values are expressed as mean ± SEM and the number of independent determinations is indicated with n.

presses the human IGF-IR. IGF-IR overexpression in murine fibroblasts is reported to result in transformation, as assayed by focus formation and tumor growth in nude mice, indicating that the NWT-21 cells would also represent a suitable IGF-IR-driven model for further in vivo efficacy studies. IGF-IR-mediated signaling was monitored both at the level of receptor autophosphorylation and phosphorylation of PKB, which is a downstream signaling event. As shown in Figure 1 and Table 3, NVP-AEW541 was capable of effectively inhibiting IGF-IR-mediated signaling, as well as cellular proliferation, in the presence of serum. In addition to phospho-IGF-IR and phospho-PKB inhibition, similar dose-dependent reduction in the level of phospho-MAPK and phospho-GSK-3β were observed in independent experiments, where NWT-21 cells were exposed in vitro to NVP-AEW541 (data not shown).

To assess and compare the activity of IGF-IR inhibitors in vivo, a pharmacodynamic model was established. Murine lung was selected as a suitable tissue based on the observation that it contains detectable levels of the receptor and that stimulation with IGF-I leads to receptor autophosphorylation and activation of downstream signaling intermediates, including PKB and MAPK. As shown in Figure 2, ligand-mediated IGF-IR autophosphorylation and phosphorylation of PKB and MAPK were abrogated upon oral administration of NVP-AEW541. Having demonstrated the ability of the compound to abrogate IGF-I signaling in vivo, its effect on subcutaneously implanted NWT-21 tumors was assessed. In line with the observations obtained in lung tissue, oral administration of NVP-AEW541 resulted in abrogation of basal and IGF-I-induced receptor, and PKB and MAPK phosphorylation in the NWT-21 tumor xenograft (Figure 3).

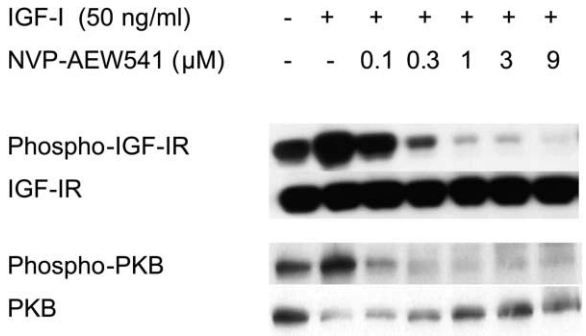

Figure 1. Inhibition of IGF-IR signaling by NVP-AEW541 in NWT-21 cells

Inhibition of IGF-IR-mediated signaling by NVP-AEW541 was determined in NWT-21 cells, a derivative of NIH3T3 mouse fibroblasts obtained upon overexpression of the human IGF-IR. Cells were grown as a monolayer, exposed to NVP-AEW541, and stimulated with IGF-I. IGF-IR and PKB phosphorylation, as well as their total protein levels, were determined by Western blot as described in the Experimental Procedures.

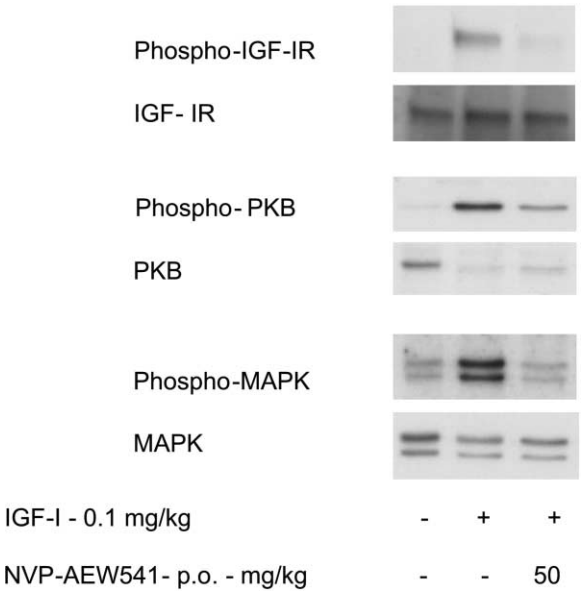

Figure 2. Inhibition of IGF-IR signaling by NVP-AEW541 in a mouse pharmacodynamic model

Inhibition of IGF-IR-mediated signaling by NVP-AEW541 in murine lung was determined ex vivo as described in the Experimental Procedures. NVP-AEW541 was administered p.o. at 50 mg/kg; one hour later, IGF-I at 0.1 mg/kg was injected i.v., and the tissue was collected 5 min thereafter. IGF-IR, PKB, and MAPK phosphorylation, as well as their total levels to ensure equal loading, were determined ex vivo by immunoprecipitation-Western blot (phospho-IGF-IR) or by Western blot.

Finally, the in vivo antitumor activity of NVP-AEW541 was assessed in the NWT-21 fibrosarcoma tumor model (Figure 4). Animals with established NWT-21 subcutaneous tumors were treated orally (bid, 7×/week) with 20 mg/kg, 30 mg/kg, or 50 mg/kg of NVP-AEW541. A consistent and dose-dependent inhibition of tumor growth was observed in compound treated animals with T/C values of 32%, 28% and 14%, respectively. All treatment groups had significantly smaller tumor volumes, as compared to the tumor volumes in the control vehicle group (Dunnett's test, $p < 0.05$). NVP-AEW541 was well tolerated at the doses applied, and the recorded variations in body weight were not statistically significant. Thus, NVP-AEW541 fulfills the requirements, in terms of potency, specificity, oral bioavailability and in vivo activity, to represent an effective IGF-IR targeting anticancer agent.

Discussion

NVP-AEW541 is an optimized IGF-IR kinase inhibitor that selectively distinguishes between the native IGF-IR and the closely related InsR. The selectivity toward the IGF-IR is observed at the cellular level (27-fold), but not in the in vitro kinase assays,

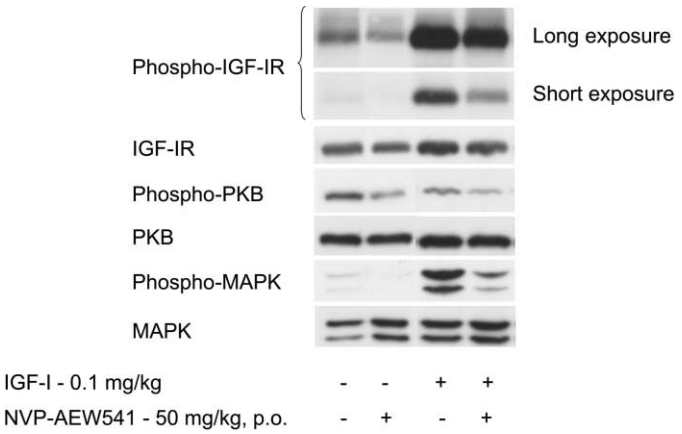

Figure 3. Inhibition of IGF-IR signaling by NVP-AEW541 in NWT-21 tumor xenografts

Inhibition of IGF-IR-mediated signaling by NVP-AEW541 in subcutaneous NWT-21 tumors was determined ex vivo as described in the Experimental Procedures. NVP-AEW541 was administered p.o. at 50 mg/kg; one hour later, tumor tissue was collected with or without prior stimulation with IGF-I (0.1 mg/kg) by i.v. injection. IGF-IR, PKB, and MAPK phosphorylation, as well as their total levels to ensure equal loading, were determined ex vivo by Western blot.

where recombinant protein fragments corresponding to the respective kinase domains are used. It is conceivable that structural features peculiar to each of these two receptors, but absent in the recombinant kinases, affect and differentiate the conformation of the respective kinase domains in the context of the native receptors. Similar observations were obtained in the case of Flt-3, where the selectivity of NVP-AEW541 toward the IGF-IR improved from 2.8-fold in vitro to 21-fold at the cellular level (data not shown).

The compound was found to fulfill the key characteristics expected from an IGF-IR inhibitor. It effectively inhibits the survival function ascribed to IGF signaling and prevents the ability of transformed cells to grow in an anchorage-independent manner, both events occurring at concentrations that are consistent with its capacity to inhibit IGF-IR autophosphorylation. In keeping with the notion that IGF-IR-mediated signaling is key for the growth of tumor cells under anchorage-independent conditions, but less so for their growth as adherent monolayer, higher concentrations of compound were generally required to inhibit proliferation of tumor cells in monolayer cultures than in the soft agar. Furthermore, cell-cell contact has been observed to negatively influence the sensitivity of cells to IGF-IR inhibitors (data not shown), probably because other, cell-contact-driven, survival mechanisms come into play. Thus, inhibition of IGF-IR signaling is likely to be more efficacious in inhibiting the onset of metastasis than the growth of an established primary tumor, unless the latter is exquisitely IGF-dependent. This view is supported by studies in which impairment of IGF-IR function, either through the use of antisense molecules or dominant negative mutants (Long et al., 1995; Dunn et al., 1998), led to a reduction in the number of metastasis, but not the primary tumor.

To first assess the in vivo antitumor efficacy of NVP-AEW541, we utilized a mechanistic IGF-IR-driven tumor model, obtained by ectopic expression of the human IGF-IR in NIH3T3 mouse fibroblasts. This cellular system was shown to respond to NVP-AEW541 in vitro in terms of both reduced proliferative capacity and IGF-IR-mediated signaling. Prior to performing the efficacy studies, NVP-AEW541 was demonstrated to strongly inhibit IGF-IR-mediated signaling in both a pharmacodynamic model and in subcutaneously implanted NWT-21 tumors. Consistently with IGF-IR signaling inhibition, NVP-AEW541 was found to significantly impair the growth of subcutaneously implanted NWT-21 tumors, thereby demonstrating the efficacy of this inhibitor toward IGF-IR driven tumors in vivo.

Despite the cellular selectivity achieved toward the IGF-IR, as compared to the InsR, there remains a potential risk of such a compound interfering with glucose/insulin metabolism. In fact, the two receptors can form heterodimers, a situation where a selective IGF-IR inhibitor would prevent crossphosphorylation and activation of the associated InsR heterodimeric partner. Alternatively, the compound could in principle accumulate at concentrations high enough to also inhibit the InsR. To assess this potential risk, plasma glucose and plasma insulin were monitored in mice treated with efficacious doses (50 mg/kg, bid, p.o.) of NVP-AEW541. No significant differences were observed when the plasma glucose and insulin levels of vehicle and com-

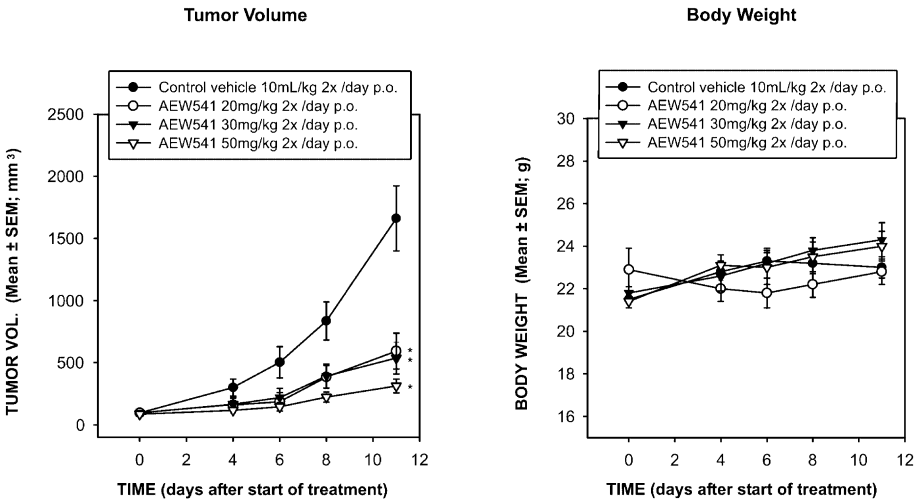

Figure 4. Inhibition of tumor growth by oral administration of NVP-AEW541 in a fibrosarcoma model

Tumors were established in female nude mice (Hsd:Athymic Nude-*nu*) by subcutaneous implantation of NWT-21 tumor fragments (3 × 3 × 3 mm) obtained from donor mice. Seven days after implantation (day 0), treatment with NVP-AEW541 was started at doses of 20 mg/kg, 30 mg/kg, and 50 mg/kg p.o. bid, 7×/week. Vehicle controls received 25 mM L(+)-tartaric acid p.o. bid, 7×/week. Tumor volumes were determined according to the formula $L \times W \times H \times \pi / 6$ and are shown in mm^3 as mean ± SEM. Body weights are shown in g as mean ± SEM. The experiment was terminated 11 days after start of treatment. *$p < 0.05$ (Dunnett's) versus control vehicle.

pound treated animals were compared after 10 days of treatment (see Supplemental Table S1 at http://www.cancercell.org/cgi/content/full/5/3/231/DC1), indicating that at least under these conditions, antitumor activity could be achieved without affecting the concentration of glucose and insulin in plasma.

Thus, NVP-AEW541 specifically targets the IGF-IR and represents a novel, potential therapeutic strategy for the treatment of tumor types for which IGF-IR-mediated signaling is a required driving/survival function. One such tumor type is likely to be multiple myeloma, for which dependency on IGF-signaling and sensitivity to a closely related IGF-IR kinase inhibitor have been demonstrated in vitro and in vivo in the accompanying manuscript (Mitsiades et al., 2004, this issue of *Cancer Cell*).

Experimental procedures

In vitro kinase assays

The protein kinases were cloned, expressed, purified, and assayed according to the following procedure unless explicitly stated otherwise. pFbacG01, pFbacGST2T, and pFbacGSTx3 Bac-to-Bac donor vectors were generated from the pFastBac1 vector (GIBCO-BRL; Cheshire, UK) by insertion of the GST coding sequence from pAcG1, pAcG2T, and pAcG3X, respectively (PharMingen; San Diego CA, USA). The kinase coding sequences were then fused to GST and sequence identity was confirmed.

Viruses for each of the kinases were generated in Sf9 (ATCC# CRL-1711) or Sf21 (ATCC# VR-2209) cells (American Type Culture Collection; Manassas, VA, USA) according to the protocol supplied by GIBCO-BRL (Cheshire, UK), unless stated otherwise.

For large-scale protein expression, 100 cm^2 round tissue culture plates were seeded with 5×10^7 cells/plate and infected with 1 ml of virus-containing media ($\sim$5 MOIs). After 3 days, the cells were scraped off the plate and centrifuged at 500 rpm for 5 min. Cell pellets from 10–20 100 cm^2 plates were resuspended in 50 ml of ice-cold lysis buffer (25 mM Tris·HCl [pH 7.5], 2 mM EDTA, 1% NP-40, 1 mM DTT, 1 mM PMSF). The cells were stirred on ice for 15 min and then centrifuged at 5000 rpm for 20 min. The clear lysate was loaded onto a 2 ml glutathione-sepharose column (Pharmacia; Dübendorf, Switzerland) and washed three times with 10 ml of 25 mM Tris•HCl (pH 7.5), 2 mM EDTA, 1 mM DTT, and 200 mM NaCl. The GST-tagged proteins were then eluted by 10 applications (1 ml each) of 25 mM Tris·HCl (pH 7.5), 10 mM reduced glutathione, 100 mM NaCl, 1 mM DTT, and 10% Glycerol, and stored at −70°C.

The activities of protein kinases were assayed in the presence or absence of inhibitors by measuring the incorporation of ^{33}P from [$\gamma^{33}P$]ATP (1000 Ci/mmol; Amersham; Little Chalfont, UK) into appropriate substrates. NVP-AEW541 was dissolved in DMSO (10 mM) and stored at −20°C. Dilutions were freshly made in DMSO/water 1:1. The final concentration of DMSO in the enzyme assays was <0.5 %. The protein kinase assays were carried out in 96-well plates at RT under conditions described in details below and terminated by the addition of 20 μl of 125 mM EDTA. Subsequently, 30 μl (c-Abl, c-Src, IGF-1R) or 40 μl (all other kinases) of the reaction mixture were transferred onto Immobilon-PVDF (Millipore; Bedford, MA, USA) presoaked for 5 min with methanol, rinsed with water, then soaked for 5 min with 0.5 % H_3PO_4 and mounted on vacuum manifold. After spotting all samples, vacuum was connected and each well rinsed with 200 μl 0.5 % H_3PO_4. Membranes were removed and washed 4× on a shaker with 1.0 % H_3PO_4, once with ethanol. After drying, mounting in Packard TopCount 96-well frame, and adding of 10 μl/well of Microscint (PerkinElmer Schweiz; Hühnenberg, Switzerland), membranes were counted. IC_{50} values were calculated by linear regression analysis of the percentage inhibition of each compound in duplicate, at four concentrations (usually 0.01, 0.1, 1, and 10 μM). One unit of protein kinase activity is defined as 1 nmole of ^{33}P transferred from [$\gamma^{33}P$]ATP to the substrate protein per minute per mg of protein at 37°C.

PKC-α

Expression of recombinant bovine PKC-α using the baculovirus system has been described (Stabel et al., 1991; Geiges et al., 1997). PKC-α was partially purified by DEAE sepharose (Pharmacia; Dübendorf, Switzerland). The enzyme assay was carried out for 20 min at RT in a final volume of 30 μl containing 0.1–0.3 U of PKC-α, 20 mM Tris•HCl (pH 7.4), 10 mM $Mg(NO_3)_2 \times 6H_2O$, 200 μg/mL Protamine sulfate, 1 % DMSO, 10 μM ATP, and 0.1 μCi [$\gamma^{33}P$]ATP (37–110 TBq/mmol).

Cdk1/cycB

The enzyme was isolated from starfish oocytes by Dr. L. Meijer (CNRS Roscoff, France). Starfish oocytes were induced to enter M phase of the cell cycle with 10 μM 1-methyladenine, frozen in liquid nitrogen, and stored at −80°C. The oocytes were then homogenized following thawing and centrifuged as described (Arion et al., 1988; Rialet and Meijer, 1991). The supernatant from oocytes was equilibrated for 30 min at 4°C under constant rotation with the $p9^{CKShs}$-sepharose beads. After extensive washing, elution of Cdk1/cycB kinase from the $p9^{CKShs}$-sepharose beads was performed with recombinant human $p9^{CKShs}$ (3 mg/ml) as described (Azzi et al., 1992). The activity of Cdk1/cycB was measured as described (Azzi et al., 1992; Meijer et al., 1989, 1991) with slight modifications. The enzyme assay was carried out for 30 min at RT in a final volume of 30 μl containing 0.1–0.3 U of Cdk1/cycB, 0.1 mg/ml histone H1 (Sigma; St. Louis, Mo., USA) as a substrate, 60 mM β-glycerophosphate, 30 mM nitrophenylphosphate, 25 mM MOPS, 5 mM EGTA (pH 8.0), 15 mM $MgCl_2$, 1 mM DTT, 0.1 mM Na_3VO_4, 1 % DMSO, 7.5 μM ATP and 0.1 μCi [$\gamma^{33}P$]ATP (37–110 TBq/mmol).

PKA

The catalytic domain of PKA was assayed according to the manufacturer's procedure (Sigma; St. Louis, Mo., USA). In brief, liophilized PKA from rabbit muscle was reconstituted in nanopure water and frozen −20°C as stock aliquots (5000 U/ml). The heptapeptide Leu-Arg-Arg-Ala-Ser-Leu-Gly, known as Kemptide (Bachem; Bubendorf, Switzerland), was used as peptide substrate. The enzyme assay was carried out for 20 min at RT in a final volume of 30 μl containing 1 U of PKA, 100 mM MES-NaOH (pH 7.0), 15 mM $Mg(OAc)_2 \times (4H_2O)$, 225 mM NaCl, 50 μM ATP (0.1 μCi [$\gamma^{33}P$]ATP (37-110TBq/mmol), 0.3 mg/ml Kemptide, 0.75 mM EDTA (pH 7.0), 3.0 mg/ml bovine serum albumin, 1 % DMSO and 10% glycerol.

c-raf-1

Production of recombinant c-Raf-1 was performed by triple infection of Sf21 cells with GST-c-Raf-1 baculovirus together with v-Src and v-Ras baculoviruses that are required for active c-Raf-1 kinase production (Williams et al., 1992). Active Ras (v-Ras) is required to recruit c-Raf-1 to the cell membrane, and v-Src is required to phosphorylate c-Raf-1 to fully activate it (Williams et al., 1992). IκB, expressed in bacteria as a His-tagged protein, was used as substrate for the c-Raf-1 kinase. Bacteria were lysed by sonication (microtip limit setting for 3 times at 1 min each) in sonication buffer (50 mM Tris·HCl [pH 8.0], 1 mM DTT, 1 mM EDTA) and centrifuged at 10,000 × g for 15 min. The supernatant was mixed with ammonium sulfate to give a final concentration of 30%. This mixture was rocked for 15 min at 4°C then spun at 10,000 g for 15 min. The pellet was resuspended in binding buffer containing 10 mM BSA. This solution was applied to Ni-agarose and washed according to the manufacturer. IκB was eluted from the column using elution buffer (8 mM Tris·HCl [pH 7.9], 0.2 M NaCl, 0.4 M imidazole). Fractions containing protein were dialyzed in 50 mM Tris·HCl (pH 8), 1 mM DTT. The enzyme assay was carried out for 45 min at RT in a final volume of 30 μl containing 750–1000 ng GST-c-Raf-1 kinase, 20 mM Tris•HCl (pH 7.5), 3.0 mM $MgCl_2$, 3.0 mM $MnCl_2$, 10 μM Na_3VO_4, 1 mM DTT, 1 % DMSO, 1.0 μM ATP (0.1 μCi/assay [γ-^{33}P]-ATP), and 3.0 μg/mL IκB.

PKB/Akt

The α isoform of human PKB/Akt was kindly provided by Dr. T. Roberts (DFCI, Boston, USA). The kinase assays were performed as described (Alessi et al., 1996) with slight modifications. The assay was carried out for 30 min at ambient temperature in a final volume of 30 μl containing 51 mM MOPS (pH 7.2), 1.05 mM DTT, 5.0 mM $MgCl_2 \times (6H_2O)$, 0.01% Triton X-100, 100 μM [$\gamma^{33}P$]ATP (0.1μCi/vial), 0.050 mM Crosstide (GRPRTSSFAEG, manufactured in-house), and 0.1–0.3 U of PKB/Akt.

HER-1, HER-2, HER4

The HER-1 and HER-2 cDNAs were kindly provided by Dr. Nancy Hynes (FMI, Basel, Switzerland). Recombinant baculovirus was generated that expresses the amino acid region 668–1210 and 676–1255 of the cytoplasmic kinase domains of human HER-1 and HER-2, respectively. The coding sequence for HER-4 kinase domain (aa 676–1308) was amplified by PCR from a human uterus cDNA library. The kinase assays with purified GST-HER-1 (3 ng), GST-HER-2 (10 ng), and GST-HER-4 (4 ng) were carried out for 15 min at RT in a final volume of 30 μl containing 20 mM Tris·HCl (pH 7.5), 10 mM $MgCl_2$, 3 mM $MnCl_2$, 0.01 mM Na_3VO_4, 1 % DMSO, 1 mM DTT, 3 μg/mL

poly(Glu,Tyr) 4:1 (Sigma; St. Louis, Mo., USA), and 2.0 μM ATP (γ-[^{33}P]-ATP 0.1 μCi).

c-Abl

The His-tagged kinase domain of c-Abl was cloned and expressed in the baculovirus/Sf9 system as described (Bhat et al., 1997). A protein of 37 kDa (c-Abl kinase) was purified by a two-step procedure over a cobalt metal chelate column followed by an anion exchange column (Pharmacia; Dübendorf, Switzerland) with a yield of 1–2 mg/l of Sf9 cells (McGlynn et al., 1992). Tyrosine protein kinase assays with purified c-Abl contained in a total volume of 30 μl: 10 ng c-Abl kinase, 20 mM Tris·HCl (pH 7.5), 10 mM $MgCl_2$, 10 μM Na_3VO_4, 1 mM DTT, 1 % DMSO, 5 μM ATP (0.07 μCi/assay [γ-^{33}P]-ATP) and 30 μg/ml Poly-AEKY (poly-Ala,Glu,Lys,Tyr-6:2:5:1; Sigma; St. Louis, Mo., USA) and were carried out for 10 min at RT.

c-Src

The baculovirus expressing full-length chicken c-Src was generated as a GST fusion protein. The assay contained in a final volume of 30 μl: 5 ng c-Src kinase, 20 mM Tris·HCl (pH 7.5), 10 mM $MgCl_2$, 0.01 mM Na_3VO_4, 1% DMSO, 1 mM DTT, 25 μg/ml poly(Glu,Tyr) 4:1 (Sigma; St. Louis, Mo., USA), 20 μM ATP (γ-[^{33}P]-ATP 0.07 μCi), and was carried out for 10 min at RT.

IGF-IR, Ins-R

The baculovirus expressing the amino acid region 950–1337 of the mature cytoplasmic domain of the human IGF-IR was generated as a GST fusion protein. Similarly, a baculovirus expressing the amino acid region 919–1343 of the cytoplasmic kinase domain of the human insulin receptor, Ins-R, was generated. Tyrosine protein kinase assays with purified GST-IGF-IR (100 ng) and GST-Ins-R (50 ng) were performed in a final volume of 30 μl containing 20 mM Tris•HCl (pH 7.6), 10 mM $MgCl_2$, 0.01 mM Na_3VO_4, 1 % DMSO, 1 mM DTT, 3 μg/ml 1.0 μM (Ins-R), and 30 μM (IGF-IR) of poly(Glu,Tyr) 4:1 (Sigma; St. Louis, Mo., USA), and 0.1 μCi ATP (γ-[^{33}P]-ATP). The assay was carried out for 20 min at RT.

KDR, Flt-1, Flk-1, Tek, c-Met, c-Kit, c-Fms, PDGFR-β, FGFR-1

Recombinant baculovirus for the KDR (aa 807–1350), Flt-1 (aa 784–1338), Flk-1 (aa 792–1367), Tek (aa 773–1124), and PDGFR-β (aa 661–1106) kinase domains fused N-terminally to GST were provided by the lab of Dr. Marmé (Klinik für Tumour Biologie, Freiburg, Germany). The coding sequences for the cytoplasmic domain of c-Kit (aa 544–976) and c-Fms (aa 538–972) were amplified by PCR from human uterus and from human bone marrow cDNA libraries (Clontech; Palo Alto CA, USA), respectively. The assays (30 μl) contained 200–1800 ng of enzyme protein (depending on the specific activity), 20 mM Tris•HCl (pH 7.6), 3 mM $MnCl_2$, 3 mM $MgCl_2$, 1 mM DTT, 10 μM Na_3VO_4, 3 μg/ml poly(Glu,Tyr) 4:1 (Sigma; St. Louis, Mo., USA), 1 % DMSO, 1.0 μM ATP (c-Met, c-Kit, c-Fms), 8.0 μM ATP (KDR, Flt-1, Flk, Tek, FGFR-1), 10.0 μM ATP (PDGFR-β) (γ-[^{33}P]-ATP 0.1 μCi), and were carried out for 10–30 min at RT.

Flt-3

Recombinant baculovirus that expresses the amino acid region 563–993 of the cytoplasmic kinase domains of human Flt-3 was generated. The coding sequences for the cytoplasmic domain of Flt-3 were amplified by PCR from human c-DNA libraries (Clontech; Palo Alto CA, USA). Tyrosine protein kinase assays with purified GST-Flt-3 was carried out for 15 min at RT in a final volume of 30 μl containing 200–1800 ng of enzyme protein (depending on the specific activity), 20 mM Tris•HCl (pH 7.6), 3 mM $MnCl_2$, 3 mM $MgCl_2$, 1 mM DTT, 10 μM Na_3VO_4, 3 μg/mL poly(Glu,Tyr) 4:1 (Sigma; St. Louis, Mo., USA), 1 % DMSO, 8.0 μM ATP (γ-[^{33}P]-ATP 0.1 μCi).

Flt-4

A fusion protein of GST and the cytoplasmic domain of human Flt-4 (GST-Flt-4) expressing the amino acid regions 725–1298 was provided by Dr. Marmé (Klinik für Tumour Biologie, Freiburg, Germany). GST-Flt-4 was assayed for 15 min at RT in a final volume of 30 μl containing 200–1800 ng of enzyme protein (depending on the specific activity), 20 mM Tris•HCl (pH 7.6), 3 mM $MnCl_2$, 3 mM $MgCl_2$, 1 mM DTT, 10 μM Na_3VO_4, 3 μg/ml poly(Glu, Tyr) 4:1 (Sigma; St. Louis, MO, USA), 1% DMSO, 8.0 μM ATP (γ-[^{33}P]-ATP 0.1 μCi).

Cell lines

NWT-21 cells are NIH3T3 mouse fibroblasts that stably overexpress the human IGF-IR and were generated as previously described (Kato et al., 1993) by Dr. Thomas Geiger (Novartis Pharma AG). The cells were passaged in DMEM high glucose, 10% FBS, and 1% Na-Pyruvate. A14 cells are NIH3T3 mouse fibroblast cells that have been stably transfected with human Ins-R cDNA (Pronk et al., 1994). The cells were cultured in DMEM medium containing 10% FCS and 1% penicillin/streptomycine. The human epidermoid carcinoma cell line A431 (ATCC CRL1555) was grown in Dulbecco's modified Eagle's medium (DMEM) supplemented with 10% fetal bovine serum, in presence of 1% sodium pyruvate and 1% penicillin/streptomycin. A31 cells (BALB/3T3 clone A31, ATCC CCL-163) were grown in DMEM high-glucose with 10% FCS, 1% L-Glutamine, and 1% penicillin/streptomycin. GIST882 cells, originally derived from a human gastrointestinal stromal tumor, were obtained from Jonathan A. Fletcher (DFCI, Boston) and cultivated in RPMI 1640, supplemented with 15% FCS, and 2 mM glutamine. These cells express a mutated kit that is constitutively activated. The murine myeloid progenitor cell line 32Dcl3 transfected with the p210 Bcr-Abl expression vector pGDp210Bcr/Abl (32D-bcr/abl) was obtained from J. Griffin (Bazzoni et al., 1996). The cells express the fusion bcr-abl protein with a constitutively active abl kinase and proliferate in an IL-3-independent manner. The cells were grown in RPMI 1640, 10% fetal calf serum, 2 mM glutamine. All cell culture reagents were purchased from Invitrogen (Basel, Switzerland).

Cellular autophosphorylation assays

96-well capture ELISAs were established to measure inhibition of either ligand-induced receptor autophosphorylation (IGF-IR, InsR, EGF-R, PDGFR) or the reduction of autophosphorylation of the constitutively active kinases (c-Kit, Bcr-Abl). For all described capture ELISAs, phoshorylated target was detected using the AP-labeled anti-phosphotyrosine Ab PY20(AP) as second Ab and the chemiluminescent AP-substrate CDPStar RTU with Emerald II.

IGF-IR

NWT-21 cells were seeded into 96-well tissue culture plates (Costar; Wohlen, Switzerland) at 5000 cells/well in complete growth medium and grown to 70%–80% confluency by incubation at 37°C, 5% CO_2. After starvation for 24 hr in DMEM, 0.5% FCS, the cells were incubated for 90 min in presence or absence of test compound followed by stimulation with IGF-I (final concentration: 10 ng/ml) for 10 min at 37°C. Subsequently, the cells were washed twice with ice-cold PBS and lysed at 4°C with 50 μl/well RIPA-buffer (50 mM Tris·HCl [pH 7.2], 120 mM NaCl, 1 mM EDTA, 6 mM EGTA, 1% NP-40, 20 mM NaF, 1 mM benzamidine, 15 mM sodium pyrophosphate, 1 mM PMSF, and 0.5 mM Na_3VO_4).

MAB 24-60 was used as capture antibody for the IGF-IR. The hybridoma line producing this anti-IGF-IR monoclonal antibody was originated by K. Siddle (University of Cambridge, Cambridge, UK) and obtained from L. Schumaker (Georgetown University, Washington, USA), and the antibody was produced and purified by conventional methods. For the ELISA, black 96-well Packard Opti Plates HTRF-96 (Packard, Zürich, Switzerland) were coated overnight with 50 μl/well 0.1 μg/ml mAB 24-60 in PBS and blocked with 3% BSA in PBST (PBS containing 0.05% Tween20). 40 μl of each cell lysate was transferred to the precoated plates, mixed with 40 μl of an alkaline phosphatase (AP) labeled anti-phosphotyrosine Ab (PY20[AP], Zymed; Basel, Switzerland), diluted to 0.2 μg/ml in RIPA buffer, and incubated overnight at 4°C. After washing (PBST) and incubation for 45 min at RT with the luminescent AP-substrate CDPStar RTU with Emerald II (90 μl/well), luminescence was measured using a Packard Top Count Scintillation Counter.

InsR

A commercial monoclonal anti-Ins-R-β-subunit antibody (Neomarkers Ab6, Basel, Switzerland) was used as a capture antibody for the insulin receptor. Black ELISA plates were coated overnight with 50 μl 0.75 μg/ml Ab6 in PBS at 4°C, washed with PBST and blocked with PBST containing 3% BSA.

5×10^3 A14 cells/well were plated on 96-well plates (Costar; Wohlen, Switzerland) in complete growth medium and incubated at 37°C, 5% CO_2 until they reached confluency. After starvation for 24 hr in DMEM without FCS, followed by incubation for 90 min in the absence or presence of test compound, the cells were stimulated with 5 μg/ml insulin for 10 min at 37°C. Immediately after stimulation, the cells were washed twice with cold PBS, and lysed at 4°C with 150 μl/well freshly prepared RIPA buffer. 50 μl of each cell lysate was transferred directly from the cell culture plate to the precoated plate and incubated overnight at 4°C. Following washing with PBST, the plates were incubated for 2 hr at RT with 50 μl/well PY20(AP), diluted 1:10000 in RIPA buffer (final concentration: 0.1 μg/ml). The final washing with PBST was followed by addition of 90 μl/well chemiluminescent AP-substrate (CDPStar RTU with Emerald II) and incubation for 45 min at RT (dark). Luminescence was measured (as counts per second, CPS) with a Packard TopCount Microplate Scintillation Counter.

HER-1

A431 cells grown close to confluency in 96 well tissue culture plates were starved for 24 hr in medium with 0.5% FBS, followed by incubation with serial dilutions of the compound for 90 min. After stimulation with a final concentration of 50 ng/ml EGF (Upstate Biotechnology; 01-102, Frankfurt, Germany) for 10 min, cells were washed and lysed in 150 μl lysis buffer. For the ELISA, 50 ng/well anti-EGFR Ab5 from NeoMarkers (MS-316-P; Basel, Switzerland) was coated to black ELISA plates.

PDGFR

A31 cells grown in 96-well tissue culture plates close to confluency were starved for 4 hr in the presence of 0.5% FCS, followed by incubation with compound in starving medium for 2 hr. Subsequently, the cells were stimulated with recombinant human PDGF BB (BACHEM, Bubendorf, Switzerland) at 50 ng/ml final concentration for 10 min followed by washing and lysis in 70 μl/well lysis buffer. For the ELISA, 50 ng/well anti-PDGF-R Receptor Type A/B antibody from Upstate Biotechnology (06-495; Frankfurt, Germany) was coated to black ELISA plate.

c-Kit

96-well tissue culture plates were treated with 1.5% gelatin solution in nanopure water for 30–60 min at 37°C prior to seeding the GIST882 cells to improve adherence and cell growth. The gelatin (EIA purity reagent; BIORAD, Reinach, Switzerland) was sterilized before use by heating (autoclave). Cells were grown close to confluency in gelatin-precoated 96-well tissue culture plates. Incubation with compound for 90 min was followed by washing and cell lysis in 100 μl/well cold lysis buffer. For the ELISA, 100 ng per well monoclonal anti-CD117 antibody (Diaclone; Besançon, France) was coated to black ELISA plates.

Bcr-Abl

200,000 32D-Bcr-Abl cells were seeded per well in 96-well round bottom tissue culture plates and treated with compound for 90 min followed by washing and cell lysis in 150 μl/well lysis buffer. For the ELISA, 50 ng/well of the rabbit polyclonal anti-abl-SH3 domain (Ab 06-466; Upstate; Frankfurt, Germany) was coated to black ELISA plates.

IGF-I survival assay

MCF-7 cells were plated in 96-well dishes at 3000 cells/well in MEM EBS, 10% FCS, 1% Glutamate, 1% Na Pyruvate, and 10 μg/ml bovine insulin (Invitrogen; Basel, Switzerland). 24 hr after plating, medium was removed and the cells were washed twice with PBS. 100 μl of serum-free medium containing IGF-1 (50 ng/ml) and 0.1% BSA was added in the presence of increasing concentrations of compound. 72 hr after treatment started, cellular viability was assayed using the Cell Titer 96R Aqueous One Solution Cell Proliferation Assay (Promega; Wallisellen, Switzerland).

Soft agar assay

MCF-7 cells were grown, as described above, and the soft agar assay was adapted to 24-well plates according to the method described previously (Freedman and Shin, 1974). NVP-AEW541 was added directly to the agar-containing medium, to final concentrations of 30 to 300 nM. The basal layer contained 0.5 ml per well of 0.8% bacto agar (Invitrogen; Basel, Switzerland) in MCF7 growth medium. The plates were covered and stored in an incubator (37°C, 5% CO_2) for at least 30 min to allow the medium to solidify before addition of the top agar layer. 5000 MCF-7 cells per well were embedded in 0.5 ml top layer of 0.4% agar in growth medium. After 3 weeks incubation at 37°C, 5% CO_2, cells were fixed, stained by crystal violet, positive colonies (diameter $>$ 40 μm) counted, and the transformation efficiency determined using a Kontron KS-400 image analysis system (Zeiss; Jena, Germany).

Western blot analysis of phospho-IGF-IR, phospho-PKB, and phospho-MAPK

IGF-IR phosphorylation was tested in log phase cells. The compound (dissolved in DMSO) was added 20 min before stimulation with IGF-I (50 ng/ml) to reach final concentrations ranging from 0.1 to 10 μM. Ten minutes thereafter, the dishes were placed on ice, cells rinsed with 10 ml cold PBS, and collected in 500 μl lysis buffer (50 mM Tris·HCl [pH 7.5], 120 mM NaCl, 20 mM NaF, 1 mM EDTA, 6 mM EGTA, 15 mM pNPP, 15 mM Sodiumpyrophosphate, 1 mM Benzamidin, 0.1 mM PMSF, 0.5 mM Vanadate, 1% NP-40). Protein concentration was determined using Coomasie R Plus Protein Assay Reagent Kit (Pierce; Lausanne, Switzerland). Between 800 μg and 1 mg of total cell lysate were incubated with 2 μg specific anti-IGF-IR (C-20; Santa Cruz; Nunningen, Switzerland) overnight at 4°C on a rotating wheel. 30 μl Protein G Sepharose (Sigma; St. Louis, Mo., USA) were then added and incubation continued for 2 hr at 4°C. The Protein G Sepharose was collected, washed three times with lysis buffer, and resuspended in SDS-gel sample buffer. Samples were loaded on 7.5% SDS gels (PAGErR Gold precast gels, Bioconcept; Allschwil, Switzerland) and Western Blot was performed using anti-phospho-Tyrosine antibody (4G10) followed by a secondary HRP-linked anti-mouse Ig antibody (NA931V, Pharmacia, Dübendorf, Switzerland). Membranes were reprobed with anti-IGF-IRβ antibody (sc-713; Santa Cruz; Nunningen, Switzerland). Alternatively, IGF-IR tyrosine phosphorylation was determined on 50 μg of total cell lysates obtained from NWT-21 cells cultured in vitro using an anti-phospho-IGF-IR antibody (407707; Calbiochem/Merck; Darmstadt, Germany), followed by a secondary HRP-coupled anti rabbit IgG antibody (NA934V; Pharmacia; Dübendorf, Switzerland).

PKB phosphorylation was determined using 20 μg of the total cell extract, resolved on 12% SDS gels (PAGErR Gold precast gels, Bioconcept; Allschwil, Switzerland). Western blot was performed using an anti-Phospho-PKB (Ser473) antibody (9271, Cell Signaling; Frankfurt, Germany) or an anti-PKB antibody (9272, Cell Signaling; Frankfurt, Germany), followed by a secondary HRP-linked anti-mouse Ig antibody (NA931V, Pharmacia; Dübendorf, Switzerland).

MAPK kinase phosphorylation was determined using an antibody specific for phosphorylated threonine 202/tyrosine 204 of p44/42 MAPK (4102, Cell Signaling; Frankfurt, Germany). The level of MAPK was monitored with a specific antibody (4101, Cell Signaling; Frankfurt, Germany).

Detection was performed using the ECL Plus western blotting detection system (Amersham biosciences; Dübendorf, Switzerland).

Proliferation assay

Between 3000 and 6000 cells/well were seeded in 96-well plates with a total media volume of 100 μl/well. Increasing concentrations of the compound were added 24 hr thereafter in quadruplicate. 72 hr later, cells were fixed by addition of 25 μl/well Glutaraldehyde (20%) and incubation for 10 min at RT. Cells were then washed 2$\times$ with 200 μl/well H_2O and 100 μl Methylene Blue (0.05%) was added. After incubation for 10 min at RT, cells were washed 3$\times$ with 200 μl/well H_2O. 200 μl/well HCl (3%) was added, and following incubation for 30 min at RT on a plate shaker, absorbance was measured at 650 nm.

Ex vivo analysis

Stimulation with IGF-I was induced by i.v. injection of the growth factor (0.1 mg/kg) 5 min prior to euthanasia. Organs and tumor specimens derived from treated animals were immediately snap frozen upon removal from the animal. Samples were pulverized in a liquid nitrogen-cooled mortar and an aliquot of approximately 50 mg placed in a dry-ice-cooled Eppendorf tube. A 10 times equivalent volume of boiling extraction buffer was added (100 mM Tris·HCl [pH 7.4], 2% SDS, 10 mM DTT, 2 mM Sodium Vanadate, 0.5 mM EDTA, 0.1 mM PMSF). Following extensive vortexing, the sample was boiled for 10 min at 95°C with occasional vigorous vortexing. Following preclearing by centrifugation at 4°C and 14,000 rpm for 15 min, the supernatant was transferred to a precooled Eppendorf and the protein concentration assayed. Immunoprecipitation and Western blot analysis were carried out as described above.

In vivo efficacy study

All experimental procedures strictly adhered to the Eidgenössisches Tierschutzgesetz and the Eidgenössische Tierschutzverordnung and were covered by the permit No. 1763 issued by the Kantonale Veterinäramt Basel-Stadt (Switzerland). Female Harlan athymic nude mice were obtained from a Novartis internal breeding population (Hsd:Athymic Nude-*nu*) and were kept under optimal hygienic conditions. The initial body weight of the animals at time of arrival was between 18 and 25 g. The animals were kept in Makrolon type III cages (8 animals per cage) in a 12 hr/12 hr light/dark cycle, and food and water were ad libitum. At the end of the experiment, animals were sacrificed by CO_2 inhalation.

Generation of NWT-21 tumor fragments and treatment of animals was performed as follows. NWT-21 cells were grown in DMEM (high glucose, 4.5 g/l), 10% FCS, 1% L-glutamine, and 1% Na-pyruvate. 5 $\times$ 10^6 cells/animal were initially injected s.c. into the right flank of five mice. For the in vivo efficacy experiment, tumors of 500 to 800 mm^3 were excised and

nonnecrotic areas were cut to fragments of 3 × 3 × 3 mm. Tumor fragments were washed in sterile PBS and one tumor fragment per animal was transplanted s.c. into the right flank. Tumor volumes (length × width × height × π / 6) and body weights were determined three times weekly. At the first day of treatment (day 0), the therapy group (NVP-AEW541) and the control group (vehicle only) were selected by stratification (8 animals per group, average tumor volume of about 95 mm^3 per group). Animals were treated p.o. twice daily, 7 days/week either with NVP-AEW541 (20, 30, or 50 mg/kg; 10 ml/kg dissolved in 25 mM L(+)-tartaric acid, therapy group) or with 25 mM L(+)-tartaric acid (control group). Antitumor activity was expressed as T/C% (mean increase of tumor volumes of treated animals divided by the mean increase of tumor volumes of control animals multiplied by 100). The experiment was terminated when the mean tumor volume was about 1500 mm^3.

Results are presented as mean ± standard error of the mean (SEM). The differences in tumor volumes and body weights were statistically analyzed using one-way ANOVA with Dunnett test. The level of significance was set at $p < 0.05$. Statistical analyses were performed using SigmaStat 2.03 (Jandel Scientific; Zürich, Switzerland).

Compound synthesis

NVP-AEW541 is a pyrrolo[2,3-*d*]pyrimidine derivative synthesized at Novartis Pharma AG, Basel, Switzerland (Capraro et al., 2002).

Acknowledgments

We would like to thank Drs. A. Fletcher, J. Griffin, N. Hynes, D. Marmé, L. Meijer, T. Roberts, and L. Schumaker for kindly providing reagents. For excellent technical assistance, we wish to thank Dorothee Arz, Sarah Barbet, Bruno Bohler, Jacqueline Bohn, Benjamin Buchs, Mario Centeleghe, Monique Ducarre, Peter Haberthuer, Roland Haller, Patrick Hauser, Thomas Huerlimenn, Claudia Koelbing, Claire Kowalik, Iris Lassoued, Nicole Martin, Kailai Nathan, Mike Oswald, Kerstin Pollehn, Veronique Rigo, Rosemarie Roth, Barabara Schacher Engstler, Christelle Stamm, Sonja Tobler, and Roman Wille.

Received: October 14, 2003
Revised: January 20, 2004
Accepted: February 5, 2004
Published online: February 26, 2004

References

Alessi, D.R., Caudwell, F.B., Andjelkovic, M., Hemmings, B.A., and Cohen, P. (1996). Molecular basis for the substrate specificity of protein kinase B; comparison with MAPKAP kinase-1 and p70 S6 kinase. FEBS Lett. *399*, 333–338.

Arion, D., Meijer, L., Brizuela, L., and Beach, D. (1988). Cdc 2 is a component of the M-phase specific histone H1 kinase: evidence for identity with MPF. Cell *55*, 371–378.

Artega, C.L., and Osborne, C.K. (1989). Growth inhibition of human breast cancer cells in vitro with an antibody against the type I somatomedin receptor. Cancer Res. *49*, 6237–6241.

Azzi, L., Meijer, L., Reed, S.I., Pidikiti, R., and Tung, H.Y.L. (1992). Interaction between the cell cycle control protein $p34^{cdc2}$ and $p9^{CKShs}$: evidence for two cooperative binding domains in $p9^{CKShs}$. Eur. J. Biochem. *203*, 353–360.

Baserga, R. (2000). The contradictions of the insulin-like growth factor 1 receptor. Oncogene *19*, 5574–5581.

Bazzoni, G., Carlesso, N., Griffin, J.D., and Hemler, M.E. (1996). Bcr/Abl expression stimulates integrin function in hematopoietic cell lines. J. Clin. Invest. *98*, 521–528.

Bhat, A., Kolibaba, K.S., Oda, T., Ohno-Jones, S., and Druker, B.J. (1997). Interactions of CBL with BCR-ABL and CRKL in BCR-ABL-transformed myeloid cells. J. Biol. Chem. *272*, 16170–16175.

Burfeind, P., Chernicky, C.L., Rinisland, F., and Ilan, J. (1996). Antisense RNA to the type I insulin-like growth factor receptor suppresses tumour growth and prevents invasion by rat prostate cancer cells in vivo. Proc. Natl. Acad. Sci. USA *93*, 7263–7268.

Capraro, H.G., Furet, P., Garcia-Echeverria, C., and Manley, P.W. (2002). 4-amino-5-phenyl-7-cyclobutyl-pyrrolo[2,3-*d*]pyrimidine derivatives. PCT International Patent Application Publication WO 02/92599.

Chernicky, C.L., Yi, L., Tan, H., Gan, S.U., and Ilan, J. (2000). Treatment of human breast cancer cells with antisense RNA to the type I insulin-like growth factor receptor inhibits cell growth, suppresses tumourogenesis, alters the metastatic potential and prolongs survival in vivo. Cancer Gene Ther. *7*, 384–395.

Coppola, D., Ferber, A., Miura, M., Sell, C., D'Ambrosio, C., Rubin, R., and Baserga, R. (1994). A functional insulin-like growth factor I receptor is required for the mitogenic and transforming activities of the epidermal growth factor receptor. Mol. Cell. Biol. *14*, 4588–4595.

D'Ambrosio, C., Ferber, A., Resnicoff, N., and Baserga, R. (1996). A soluble Insulin-like growth factor I receptor that induces apoptosis of tumour cells in vivo and inhibits tumourogenesis. Cancer Res. *56*, 4013–4020.

De Angelis, T., Ferber, A., and Baserga, R. (1995). R. Insulin-like growth factor I receptor is required for the mitogenic and transforming activities of the platelet-derived growth factor receptor. J. Cell. Physiol. *164*, 214–221.

De Leon, D.D., Wilson, D.M., Powers, M., and Rosenfeld, R.G. (1992). Effects of insulin-like growth factors (IGFs) and IGF receptor antibodies on the proliferation of human breast cancer cells. Growth Factors *6*, 327–336.

Dunn, S.E., Ehrlich, M., Sharp, N.J.H., Reiss, K., Solomon, G., Hawkins, R., Baserga, R., and Barrett, J.C. (1998). A dominant negative mutant of the insulin-like growth factor-I receptor inhibits the adhesion, invasion and metastasis of breast cancer. Cancer Res. *58*, 3353–3361.

Freedman, V.H., and Shin, S.I. (1974). Cellular tumourigenicity in nude mice: correlation with cell growth in semi-solid medium. Cell *3*, 355–359.

Fürstenberger, G., and Senn, H.-G. (2002). Insulin-like growth factors and cancer. Lancet Oncol. *3*, 298–302.

Geiges, D., Meyer, T., Marte, B., Vanek, M., Weissgerber, G., Stabel, S., Pfeilschifter, J., Fabbro, D., and Huwiler, A. (1997). Activation of PKC subtypes α,γ,δ,ϵ,ζ and η by tumour promoting and non-tumour promoting agents. Biochem. Pharmacol. *53*, 865–875.

Grimberg, A., and Cohen, P. (2000). Role of insulin-like growth factors and their binding proteins in growth control and carcinogenesis. J. Cell. Physiol. *183*, 1–9.

Kalebic, T., Blakesley, V., Slade, C., Plasschaert, S., Leroith, D., and Melman, L.J. (1998). Expression of a kinase deficient IGF-IR suppresses tumourogenicity of rhabdomyosarcoma cells constitutively expressing a wild-type IGF-IR. Int. J. Cancer *76*, 223–227.

Kaleko, M., Rutter, W.J., and Miller, A.D. (1990). Overexpression of the human insulin-like growth factor I receptor promotes ligand dependent neoplastic transformation. Mol. Cell. Biol. *10*, 464–473.

Kato, H., Faria, T.N., Stannard, B., Robverts, C.T., and LeRoith, D. (1993). Role of tyrosine kinase activity in signal transduction by the insulin-like growth factors (IGF-I) receptor. J. Biol. Chem. *268*, 2655–2661.

Khandwala, H.M., McCutcheon, I.E., Flyvbjerg, A., and Friend, K.E. (2000). The effects of insulin-like growth factors on tumourogenesis and neoplastic growth. Endocr. Rev. *21*, 215–244.

Li, W., Hyun, T., Heller, M., Yam, A., Flechner, L., Pierce, J.H., and Rudikoff, S. (2000). Activation of insulin-like growth factor I receptor signaling pathway is critical for mouse plasma cell tumour growth. Cancer Res. *60*, 3909–3915.

Long, L., Rubin, R., Baserga, R., and Brodt, P. (1995). Loss of the metastatic phenotype in murine carcinoma cells expressing an antisense RNA to insulin-like growth factor receptor. Cancer Res. *55*, 1006–1009.

Lopez, T., and Hanahan, D. (2002). Elevated levels of the IGF-I receptor convey invasive and metastatic capability in a mouse model of pancreatic islet tumourogenesis. Cancer Cell *1*, 339–353.

McGlynn, E., Becker, M., Mett, H., Reutener, S., Cozens, R., and Lydon, N.B. (1992). Large scale purification and characterization of a recombinant

epidermal growth factor receptor protein tyrosine kinase. Eur. J. Biochem. *207*, 265–275.

Mitsiades, C.S., Mitsiades, N.S., McMullan, C.J., Poulaki, V., Shringarpure, R., Akiyama, M., Hideshima, T., Chauhan, D., Joseph, M., Libermann, T.A., et al. (2004). Inhibition of the insulin-like growth factor receptor-1 tyrosine kinase activity as a therapeutic strategy for multiple myeloma, other hematologic malignancies, and solid tumors. Cancer Cell *5*, this issue, 221–230.

Meijer, L., Arion, D., Golsteyn, R., Pines, J., Brizuela, L., Hunt, T., and Beach, D. (1989). Cyclin is a component of the sea urchin egg M-Phase specific histone H1 kinase. EMBO J. *8*, 2275–2282.

Meijer, L., Azzi, L., and Wang, J.Y.J. (1991). Cyclin B targets $p34^{cdc2}$ for tyrosine phosphorylation. EMBO J. *8*, 2275–2282.

Nakamura, K., Hongo, A., Kodama, J., Miyagi, Y., Yoshinuchi, M., and Kudo, T. (2000). Down-regulation of the insulin-like growth factor I receptor by antisense RNA can reverse the transformed phenotype of human cervical cancer cell lines. Cancer Res. *60*, 760–765.

Prager, D., Li, H.L., Asa, S., and Melmed, S. (1994). Dominant negative inhibition of tumourogenesis *in vivo* by human insulin-like growth factor I receptor mutant. Proc. Natl. Acad. Sci. USA *91*, 2181–2185.

Pronk, G.J., de Vries-Smits, A.M., Buday, L., Downward, J., Maassen, J.A., Medema, R.H., and Bos, J.L. (1994). Involvement of Shc in Insulin- and Epidermal Growth Factor-induced activation of $p21^{ras}$. Mol. Cell. Biol. *14*, 1575–1581.

Resnicoff, M., Coppola, D., Sell, C., Rubin, R., Ferrone, S., and Baserga, R. (1994). Growth inhibition of human melanoma cells in nude mice by antisense strategies to type 1 insulin-like growth factor receptor. Cancer Res. *54*, 4848–4850.

Resnicoff, M., Burgaud, J.L., Rotman, H.L., Abraham, D., and Baserga, R. (1995). Correlation between apoptosis, tumourogenesis and the levels of insulin-like growth factor I receptor. Cancer Res. *55*, 3739–3741.

Reiss, K., D'Ambrosio, C., Tu, X., Tu, C., and Baserga, R. (1998). Inhibition of tumour growth by a dominant negative mutant of the insulin-like growth factor I receptor with a bystander effect. Clin. Cancer Res. *4*, 2647–2655.

Rialet, V., and Meijer, L. (1991). A new screening test for antimitotic compounds using universal M phase-specific protein kinase, $p34^{cdc2}$/cyclin B^{cdc13}, affinity-immobilized on $p13^{suc1}$-coated microtitration plates. Anticancer Res. *11*, 1581–1590.

Samani, A.A., Fallavollita, L., Jaalouk, D.E., Galipeau, J., and Brodt, P. (2001). Inhibition of carcinoma cell growth and metastasis by a vesicular stomatitis virus G-pseudotyped retrovector expressing type I insulin-like growth factor receptor antisense. Hum. Gene Ther. *12*, 1969–1977.

Scotlandi, K., Benini, S., Nanni, P., Lollini, P.L., Nicoletti, G., Landuzzi, L., Serra, M., Manara, M.C., Picci, P., and Baldini, N. (1998). Blockage of insulin-like growth factor I receptor inhibits the growth of Ewing's sarcoma in athymic mice. Cancer Res. *58*, 4127–4131.

Scotlandi, K., Avnet, S., Benini, S., Manara, M.C., Serra, M., Cerisano, V., Perdichizzi, S., Lollini, P.L., De Giovanni, C., Landuzzi, L., and Picci, P. (2002a). Expression of an IGF-I receptor dominant negative mutant induces apoptosis, inhibits tumourogenesis and enhances chemosensitivity in Ewing's sarcoma cells. Int. J. Cancer *101*, 11–16.

Scotlandi, K., Maini, C., Manara, M.C., Benini, S., Serra, M., Cerisano, V., Strammiello, R., Baldini, N., Lollini, P.L., Nanni, P., et al. (2002b). Effectiveness of insulin-like growth factor I receptor antisense strategy against Ewing's sarcoma cells. Cancer Gene Ther. *9*, 296–307.

Sell, C., Rubini, M., Rubin, R., Liu, J.P., Efstratiadis, A., and Baserga, R. (1993). Simian virus 40 large tumour antigen is unable to transform mouse embryonic fibroblasts lacking type I Insulin-like growth factor receptor. Proc. Natl. Acad. Sci. USA *90*, 11217–11221.

Sell, C., Dumenil, G., Deveaud, C., Miura, M., Coppola, D., De Angelis, T., Rubin, R., Efstratiaids, A., and Baserga, R. (1994). Effect of a null mutation of the insulin-like growth factor I receptor gene on growth and transformation of mouse embryo fibroblasts. Mol. Cell. Biol. *14*, 3604–3612.

Shapiro, D.N., Jones, B.G., Shapiro, L.H., Dias, P., and Houghton, P.J. (1994). Antisense-mediated reduction in insulin-like growth factor-I receptor expression suppresses the malignant phenotype of a human alveolar rhabdomyosarcoma. J. Clin. Invest. *94*, 1235–1242.

Stabel, S., Schaap, D., and Parker, P.J. (1991). Expression of protein kinase C isotypes in baculovirus vectors. Methods Enzymol. *200*, 670–673.

Stiles, C.D., Capone, G.T., Scher, C.D., Antoniades, H.N., Van Wyk, J.J., and Pledger, W.J. (1979). Dual control of cell growth by somatomedins and platelet-derived growth factor. Proc. Natl. Acad. Sci. USA *76*, 1279–1283.

Ullrich, A., and Schlessiger, J. (1990). Signal transduction by receptors tyrosine kinase activity. Cell *61*, 203–212.

Valentinis, B., Morrione, A., Taylor, S.J., and Baserga, R. (1997). Insulin-like growth factor I receptor signaling in transformation by Src oncogenes. Mol. Cell. Biol. *17*, 3744–3754.

Van der Geer, P., Hunter, T., and Lindberg, R.A. (1994). Receptor protein-tyrosine kinases and their signal transduction pathways. Annu. Rev. Cell Biol. *10*, 251–337.

Wang, Y., and Sun, Y. (2002). Insulin-like growth factor receptor-1 as an anti-cancer target: blocking transformation and inducing apoptosis. Curr. Cancer Drug Targets *2*, 191–207.

White, P.J., Fogarty, R.D., Werther, G.A., and Wraight, C.J. (2000). Antisense inhibition of IGF-I receptor expression in HaCaT keratinocytes: a model for antisense strategies in keratinocytes. Antisense Nucleic Acid Drug Dev. *10*, 195–203.

Williams, N.G., Roberts, T.M., and Li, P. (1992). Both $p21^{ras}$ and $pp60^{v\text{-}src}$ are required, but neither alone is sufficient, to activate the Raf-1 kinase. Proc. Natl. Acad. Sci. USA *89*, 2922–2926.

Yu, H., and Rohan, T. (2000). Role of the insulin-like growth factor family in cancer development and progression. J. Natl. Cancer Inst. *92*, 1472–1489.